Experimental and Numerical Evaluation of Reinforcement Mechanism of Geocells

Sireesh Saride (Corresponding Author)
Associate Professor,
207, Academic Block A,
Department of Civil Engineering,
Indian Institute of Technology Hyderabad, Telangana-502285, India,
Tel: +91 40 2301 6066, Email: sireesh@iith.ac.in.

Anu M George
Former Masters' student, IIT Hyderabad
Currently PhD scholar at the University of Texas at Arlington, USA
Email: anumuthumala.george@mavs.uta.edu

Vinay Kumar V
Doctoral student,
Department of Civil Engineering,
Indian Institute of Technology Hyderabad, Telangana-502285, India,
Email: christite.vinay@gmail.com

Anand J Puppala
Professor of Department of Civil Engineering
The University of Texas at Arlington, USA
Email: anand@uta.edu

Word count: 242 words text (abstract) + 3374 words text (body) + 564 words text (references) + 12 tables/figures x 250 words (each) = 7180 words

Submission date: 31/07/2016; Resubmission date: 15/11/2016

ABSTRACT

Geocells is a commonly adopted reinforcement element for foundation and pavement applications. The geocell offers confinement to the infill material in addition to the lateral restraint and bearing support as a reinforcement mechanism. However, quantification of the confinement effect offered by the geocell is a challenge.

To quantify and demonstrate the geocell's confinement mechanism, an extensive experimental and numerical studies were undertaken. In the experimental study, a large test tank was adopted to build test sections with and without geocell reinforced granular bases over weak subgrades. Several earth pressure cells were installed along the interface of the geocell reinforced base and weak subgrade layers, and within the geocell pockets. A monotonic loading was applied to understand the behavior of the geocell mattress.

The actual three dimensional honeycomb shape of the geocells was modeled using Fast Lagrangian Analysis of Continua in 3D (FLAC3D), and the geocell-soil interaction was studied from the stresses mobilized within the geocell mattress. The numerical models have predicted the experimental pressure-rut responses with about 95% accuracy. It was observed that the confining stress in the geocell mattress is not uniform throughout the mattress, rather, it decreases linearly from the point of load application. The maximum confining stress is noticed at a height ratio h/D of 0.4 under the loading region. As high as 40 kPa of confining stress is mobilized in the geocell mattress under the loading with a highest confining pressure of 194 kPa in the infill soil.

***Keywords**: Geocell, Numerical modeling, FLAC 3D, Geocell-soil Mechanism, Confining stress.*

INTRODUCTION AND BACKGROUND

The use of geosynthetics in the form of three dimensional confinement known as *geocells* has been widely used in the construction of pavements, slopes, retaining walls and foundations because of their advantages over two dimensional planar reinforcement. Geocells offer faster, cheaper, sustainable, environmental friendly solutions for the complex geotechnical problems (*1*). Numerous experimental and field studies were conducted on geocells to explore the reinforcement function. Researchers includes Rea and Mitchell (*2*), Rajagopal (*3*), Krishnaswamy et al. (*4*), Dash et al. (*5*), Weseloo (*6*), Sitharam et al. (*7*), Latha et al. (*8*), Pokharel et al. (*9*), Hegde and Sitharam (*10*) performed a series of laboratory scale tests on geocell reinforced soil beds to evaluate the performance of the geocell reinforcement using extensive instrumentation.

The numerical modeling of geocell reinforcement has been a big challenge because of its complex three dimensional honeycombed structure. Earlier, Latha and Rajagopal (*11*) have used equivalent composite approach to model the geocell reinforced soil layers, where the confining pressure within the geocell ($\Delta\sigma_3$) was assumed uniform. Even though the approach was simple, it was unrealistic to model the geocell as an equivalent soil layer. Subsequently, Han et al. (*12*) and Saride et al. (*13*) have modeled diamond and square shape of geocell respectively for pavement and foundation applications. These models were realistic, but the stress concentration at the corners resulted in underestimating the performance of the geocell reinforced soil beds. Later, Yang et al. (*14*) and Hegde and Sitharam (*15*) modeled the actual honeycombed shape of geocell by digitizing the coordinates from the photograph of a single geocell.

Based on both experimental and numerical studies, researchers have inferred that the planar reinforcements improve the performance of the reinforced sand bed by three mechanisms- by providing lateral restraint, by increasing the bearing capacity and by developing an additional membrane tension support under loading. In the case of geocell, which possess a three dimensional honeycombed structure, there exists an additional lateral confinement on the infill material, thereby improving the performance of the reinforced sand bed to a greater extend.

There have been some exceptional research in the area of geocell reinforcement in the recent years (*4, 5, 13 – 16*) and the use of geocells as a reinforcement material has gained momentum over the years. Even though the numerical modeling of geocell reinforcement has been done by researchers like Yang et al. (*14*) and Hegde and Sitharam (*15*), there are no studies available which have focused on the actual confining mechanism of the geocell reinforcement. The current paper focuses on the confining effect of the geocell reinforced dense layers over weak subgrades by evaluating the stresses developed within the geocell mattress and the infill material through a series of experimental and numerical studies.

EXPERIMENTAL STUDIES

A series of large scale static load tests were performed on unreinforced and geocell reinforced dense granular layers to evaluate the performance of the geocell reinforcement. Dry river sand was used to prepare the dense sand layer over weak subgrades. The sand can be classified as a poorly graded sand (SP) according to the American Society for Materials and Testing as the coefficient of uniformity, C_u was 2.4 and the Coefficient of curvature, C_c was 1.01. The specific gravity of sand was 2.65. High density polyethylene (HDPE) type geocells with a density ranging between 0.935-0.965 g/cm^3 and having welds at a regular interval of 400 mm were used. A square shaped geocell mattresses of width,

0.6 m and height, 0.2 m, having eight cells in honeycomb format, were adopted in all the tests. The size of the mattress was selected based on the past experience (*13, 17, 18*). The junction/weld being a weakest link in the geocell mattress, loading was directly applied on the center of the weld.

The weak sand subgrades with a relative density, R_D of 30% and a overlying dense sand base layer with an R_D of 75% were prepared in a test tank of size 1m × 1 m ×1 m (length x width x height) using a pluviation technique. In the case of geocell reinforced sand beds, the mattress was spread on the subgrade and continued to fill the base layer with in the geocells using the pluviation technique. A 150 mm diameter (D) and 15 mm thickness rigid steel plate was used to apply monotonic loading until to reach a 15 mm (10% of the plate diameter) rut depth on the surface. The size of the plate was chosen in such a way that the results are unaffected by the boundary conditions (B/D = 6.66) of the test bed. Loading was applied through a 100 kN capacity actuator which was attached to a 3.5 m high, 20 ton capacity reaction frame. The schematic of test bed with all the instrumentation used in the study is presented in Figure 1.

Linear variable differential transformers (LVDT's) with 100-mm travel and 0.001% accuracy were used to measure the rutting on the surface and one LVDT is placed in-line with the actuator. Strain gage type total earth pressure cells (EPCs) of capacities 200 kPa and 500 kPa to measure the vertical pressure at the interface of the dense and weak layers were used. Five EPCs were placed at a distance of X/D = 0, 1 and 2 from the centerline of the loading plate on either side, where X is measured from the centerline as shown in Figure 2. Another set of EPC's of capacity 100 kPa were placed within the geocell pockets at locations denoted as L1, L2, and L3 in Figure 2 to attempt to measure the confining effect of the geocell mattress. A universal data acquisition (DAQ) system was used to collect the data from the instrumentation. The data collected included applied pressure, rut depth (represented as *r*), and vertical pressure at the interface of the dense and weak layers and confining pressure within the geocell mattress. To generalize the results, the data are normalized with reference to the width of the plate (D) as rut depth ratio (r/D), height and width ratios of the geocell mattress as h/D and b/D, respectively.

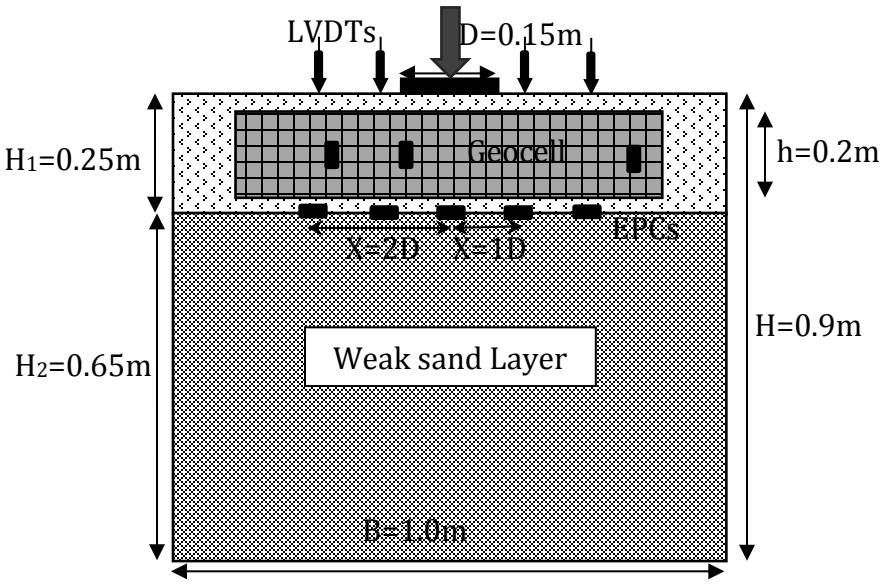

FIGURE 1: Schematic of geocell reinforced dense sand over weak sand subgrade

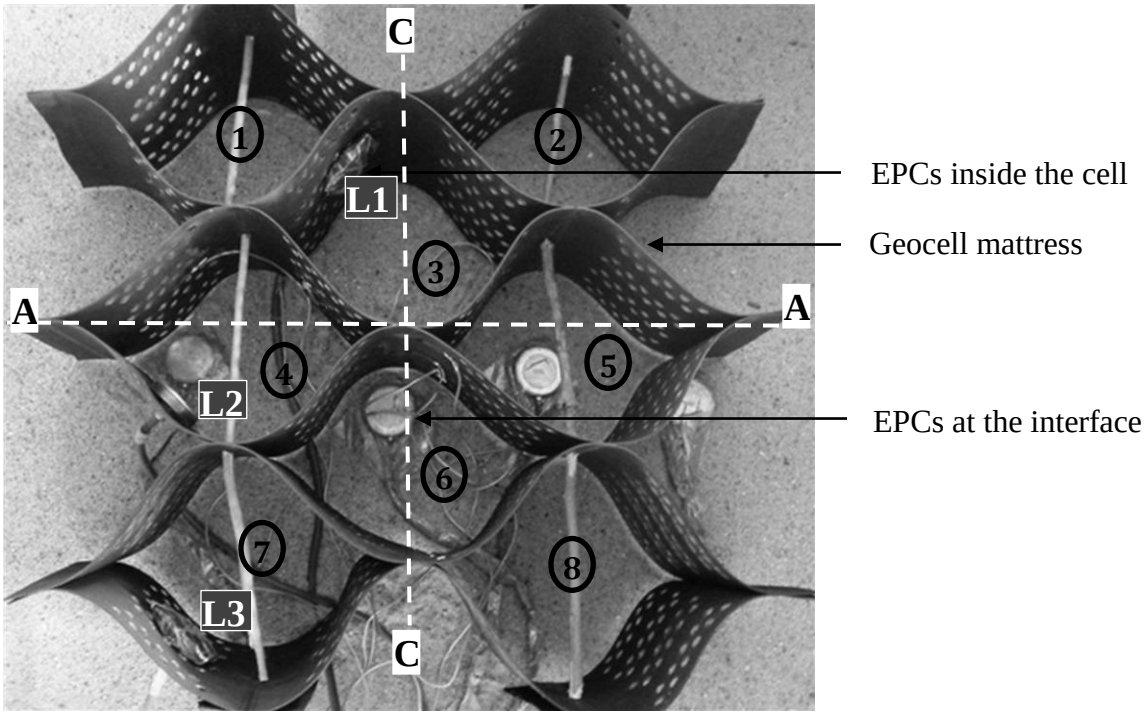

FIGURE 2: Pictorial view of the instrumentation with in the geocell mattress

NUMERICAL SIMULATIONS

Numerical simulations were carried out using a finite difference software FLAC 3D to study the confining mechanism of the geocell reinforcement in a dense sand layer over weak sand subgrade under monotonic loading conditions. To perform this, numerical models were developed to simulate the large scale experimental tests to the scale.

Numerical mesh and boundary conditions

To simulate the large-scale laboratory test sections of size 1m × 1m × 0.9m (height) a primitive mesh shape *radcylinder*, which is a radially graded mesh around the cylindrical-shaped loading plate was adopted. The radial cylinder mesh type was chosen to ensure the compatibility between the loading plate and the pavement layers. The soil model consisted of 47400 zones and the loading plate with 600 zones.. The lateral displacements were fixed at all four sides of the model and the displacement of the bottom boundary was restricted in all directions. A velocity boundary ($v=2.5*10^{-6}$ m/step) was applied at the top of the sand at a circular area having a diameter of 0.15 m. The model was solved until the settlement at the surface of the soil layer reached 30 mm, i.e. 20% rut depth. In geocell reinforced case, the actual geometry of the geocell was modelled first, by placing geogrid elements on semicircular soil zones modeled using cylindrical mesh, there by maintaining the actual curvature of the geocell pockets, and then positioned it using co-ordinates at a clearance of 0.015 m from the surface of the test section. The numerical model of geocell reinforced sand bed is shown in the Figure 3.

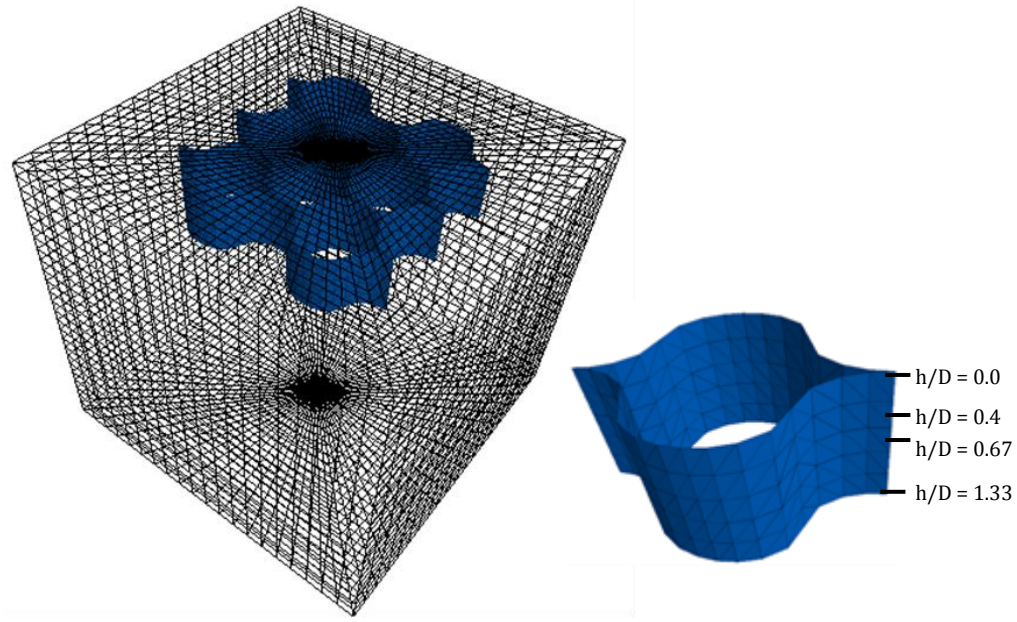

FIGURE 3 Geometry of geocell reinforced sand bed model in FLAC 3D

Material models and parameters

To represent the behaviour of two layered sand test sections in the numerical model, an elastic-perfectly plastic Mohr-Coulomb model was employed. The shear strength properties (c and ϕ) of the sand were determined from the consolidated undrained triaxial compression tests. The initial modulus of elasticity (E_1) of the top dense sand layer (R_D= 75 %) was determined using Burmister's elastic layer theory by knowing the modulus of weak sand layer (R_D = 30%), E_2 (of layer 2) from the unreinforced tests. The parameters used for in the simulations are presented in the Table 1.

Table 1 Material properties of sand and loading plate used in FLAC 3D

Properties	75 % R_D Sand	30 % R_D Sand	Plate
Bulk modulus (Pa)	5.0e6	1.8e6	1.4e11
Shear modulus (Pa)	3.0e6	0.8e6	8.04e10
Friction angle (degree)	40	30	-
Cohesion (kPa)	2.2	0.7	-
Dilation (degree)	8	0.1	-
Density (kg/m^3)	1740	1630	7.8e3

Numerical model validation

The response between the applied pressure and rut depth ratio (r/D) is compared with the experimental results for validating the numerical models. Figure 4 depicts the comparison of numerical and experimental results. It can be noticed that the numerical models have very well simulated the pressure-rut response of the unreinforced and geocell reinforced sand test sections with 95% accuracy. Notice that the geocell reinforcement has improved the load carrying capacity of the base layer by about 25%, 40% and 55% at 3%, 5% and 10% rut depth ratios, respectively. An increase in stiffness of the bed with geocell

reinforcement can be noticed. The increase in the performance can be attributed to an increased flexural rigidity of the geocell reinforced bed. The increase in the rigidity is expected to mobilize from the additional confining effect of the geocell mattress to the infill granular material.

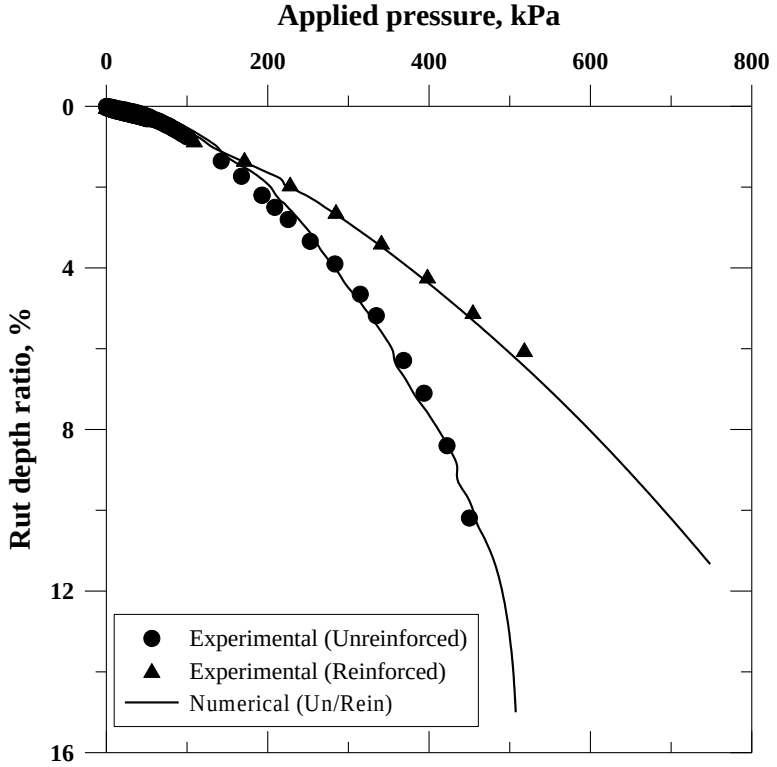

FIGURE 4 variation of applied pressure with rut depth ratio for unreinforced and geocell reinforced sections – A comparison

RESULTS AND DISCUSSIONS

After validating the numerical models with the experimental data, results obtained from the models were further analyzed for the horizontal and vertical stress distribution within the geocell and on the infill soil; and geocell coupling stresses, and compared with the measured data from the experiments.

Horizontal Stress in infill soil

Figure 5 depicts the variation of horizontal stress in the unreinforced test section in vertical cross section. A maximum horizontal stress of 61.4 kPa has been mobilized in the unreinforced bed at the centreline of loading. The magnitude of horizontal stress decreased linearly outward from the loading region.

Figure 6 shows the variation of horizontal stresses in the infill soil along the x - direction at mid height of the geocell in a plan view. A maximum horizontal stress of 116.5 kPa is noted in the geocell-pockets 3 and 6, which are located directly below the loading plate. It can also be observed that the horizontal stresses are mostly concentrated within the four geocell-pockets adjacent to the loading plate. It can be seen that the horizontal stress in the cell pockets 1, 2, 7 and 8 (as seem in Fig. 2) are negligible, and hence the

confining effect. The variation of horizontal stress along the vertical cross-section A-A is presented in Figure 7. It can be observed that highest stress developed is at an h/D ratio of 0.4 from the top of the geocell with a magnitude of about 194 kPa. It can be seen from the Figure 7 that the horizontal stress distribution is non-uniform throughout the cells, rather, it varies linearly within the cell from a highest value at the centerline of the loading to a lowest value on the opposite cell wall. It can also be noted that the horizontal stress is maximum at the mid height of the cell pockets, however, higher stresses can be noted at the bottom portion of the outer cells (nos. 1, 2, 7 and 8). The additional horizontal stresses mobilized in the infill soil is mainly due to the provision of geocell mattress. As high as two fold increase in horizontal stress is mobilized in the geocell reinforced sands against unreinforced sand section. The increase in the horizontal stress is purely due to the lateral confinement offered by the geocell mattress to the infill soil.

As the geocell mattress offers resistance to the horizontal movement (lateral confinement), which varies across the cell pockets in x-, y- and z- directions, it is also possible to observe the vertical stress distribution on the weak subgrades. It can also be deduced from the Figure 7 that the vertical stress is distributed at an angle of about 50^{o} to the horizontal or about 40^{o} to the vertical, which works out to be about 1.2:1 (V:H). This is also referred to as the load distribution angle. This effect is further analyzed in the following sections.

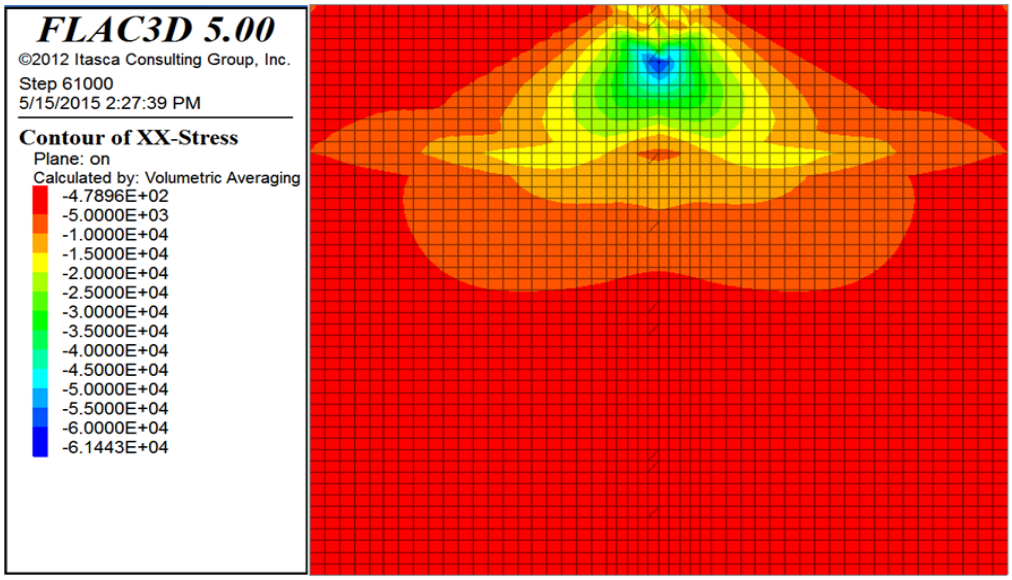

FIGURE 5 Horizontal stress in unreinforced bed – Sectional view

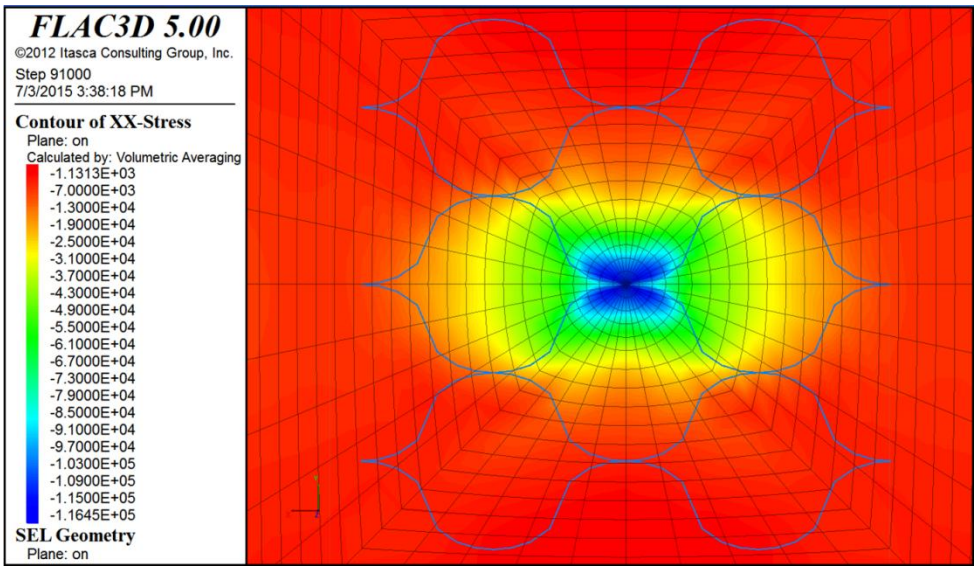

FIGURE 6 Horizontal stress in x-direction at the mid height of geocell (A-A)-Plan view

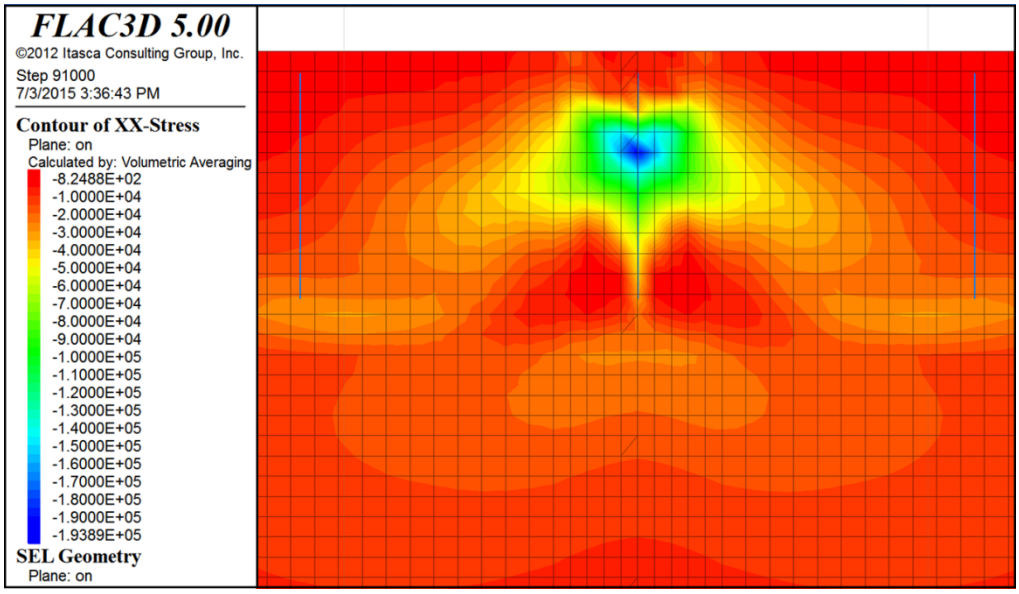

FIGURE 7 Horizontal stress in x-direction at vertical cross-section A-A-Geocell reinforced bed

Vertical pressure distribution at the interface

Figure 8 depicts the vertical pressure distribution on the weak subgrade (at the interface) due to monotonic load on the unreinforced and geocell reinforced dense sand layers. The test data is presented for 5% rut depth. A maximum pressure of about 360 kPa has been applied on the unreinforced section before it has shown the failure. An applied pressure of 510 kPa is reached on the geocell reinforced sand beds before reaching the 5% rut depth. The predicted values are in agreement with the measured vertical pressures at the interface.

It can be inferred that about 80% and 92% reduction in the vertical pressure at the interface due to dense sand layer without and with geocell mattress, respectively. However, it is important to note that the applied pressure is much lower (about 40%) in the case of unreinforced bed at 5% rut depth. It can be said that higher applied stress is transmitted to the weak subgrade in the case of unreinforced condition than the reinforced condition.

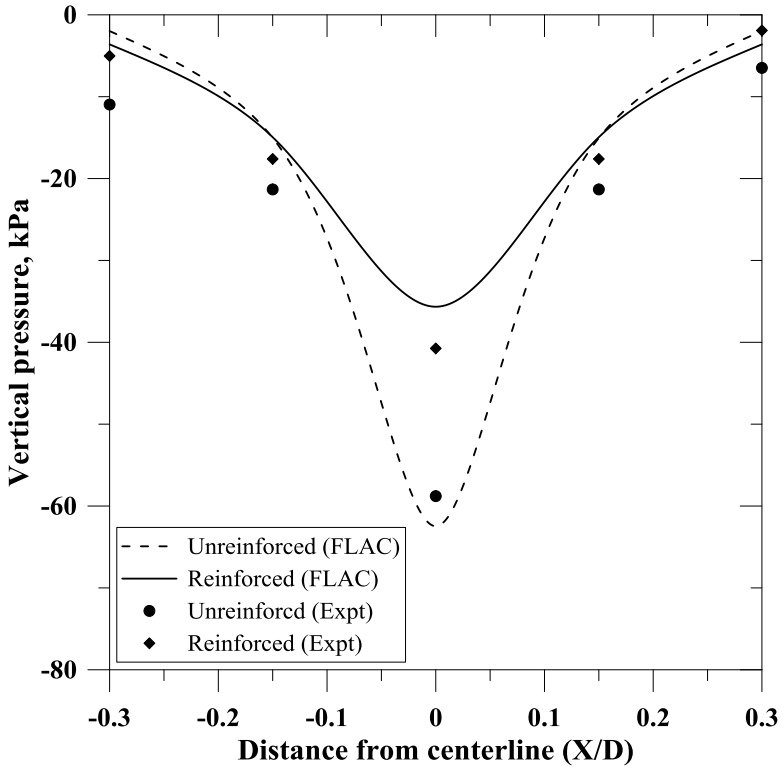

FIGURE 8 Vertical pressure distribution at the interface

Horizontal confining stress variation in the infill soil with depth

For plotting the variation of horizontal confining stress in the infill soil with depth of the geocell, four locations were selected at h/D of 0, 0.4, 0.67 and 1.33 as marked in Figure 3. The horizontal confining stress in the infill soil is collected at these locations by slicing the geocell model at the planes corresponding to the height ratios. The variation of horizontal confining stress in the geocell wall along section A-A in terms of area diagrams is shown in Figure 9. It can be observed that the horizontal confining stress is observed maximum near the centre of the loading and it gradually reduces towards the edge of the cell. The maximum horizontal confining stress of about 170 kPa has mobilized at the level of h/D ratio of 0.4. This observation is in-line with the data presented in terms of the horizontal stresses depicted in the Figures 6 and 7. The negative sign indicates the compressive nature of the stresses.

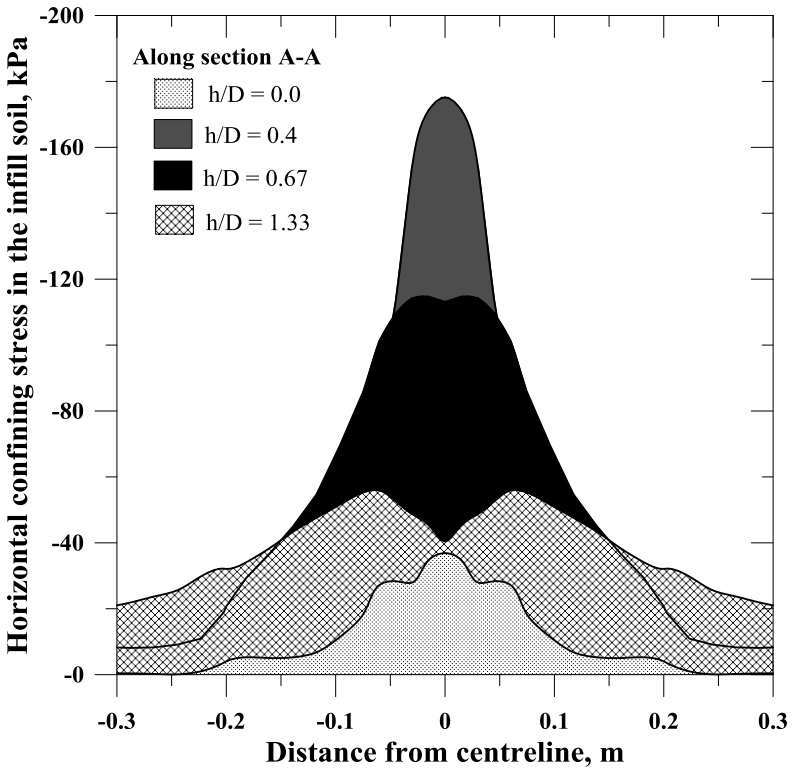

FIGURE 9 Variation of horizontal confining stress in the infill soil across A-A at various h/D ratios

Confining mechanism of geocell reinforcement

To study the actual stresses mobilized within the geocell walls under monotonic loading, three locations were selected, exactly at the same locations where the physical measurements were made in the large scale tests, as shown in the Figure 10 (inset). These locations were selected in such a way that the information from each cell recorded to develop an understanding the behavior of the entire mattress. It can be noticed that the confining stresses mobilized within the geocell mattress increased with an increase in the applied stress at all locations. However, the confining stress mobilized at the location L1 is higher than the other two locations, owing to its proximity to the loading region. It can be clearly noted that the mobilized confining stresses within the geocell in the numerical studies are close to the stresses directly measured in the large scale experiments through in-cell EPCs. The predicted values are fairly matching with the measured vertical stresses at the interface as well. The variation in the measurements may be due to the material models adopted in the numerical study. However, the numerical models have very closely predicted the pressure-rut behavior. Hence, this data validates the numerical models. Besides, the EPCs could not be placed right below the loading region due to expected potential damage to the EPCs during the test. However, the same data can now be obtained from the validated numerical models to understand the overall behavior of the geocell reinforcement.

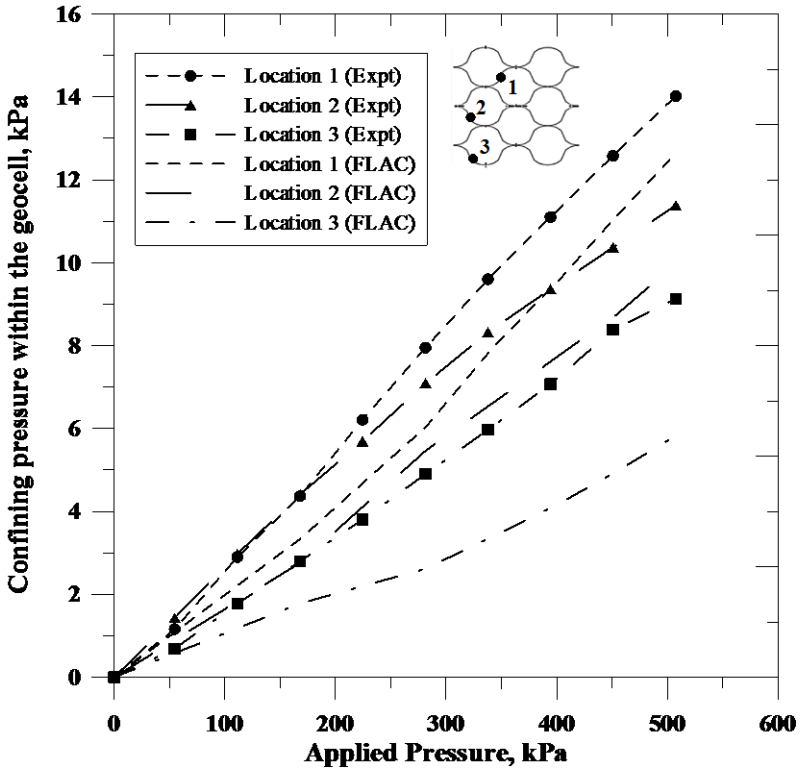

FIGURE 10 Confining pressure developed in the geocell wall – Comparison of measured and predicted values

It is always postulated that the stress mobilized within the geocells is constant throughout the section (*20-22*) in calculating the enhanced shear strength properties of the geocell reinforced composite sections. However, it is inferred from the previous sections that the mobilization of horizontal stresses, vertical stresses and the corresponding stresses developed within the geocell mattress are non-uniform across the mattress, having a highest value close to the loading region and decreases with a distance from the loading point. The confining stress acting perpendicular to the geocell wall was computed at each geogrid-sel node and was plotted as shown in Figure 11. As the load was directly acting at the centre weld of the geocell mattress with eight cells around, the maximum stress of about 40 kPa was developed at this point. The confining stress within the geocell mattress gradually decreased with an increase in the distance from the loading point. This is because of the development of higher stresses in the infill soil during the loading, which will in-turn results in the mobilization of higher confining stresses in the geocell mattress. Hence, for the design applications a linearly decreasing confining pressures within the cell pockets may be considered from the point of loading.

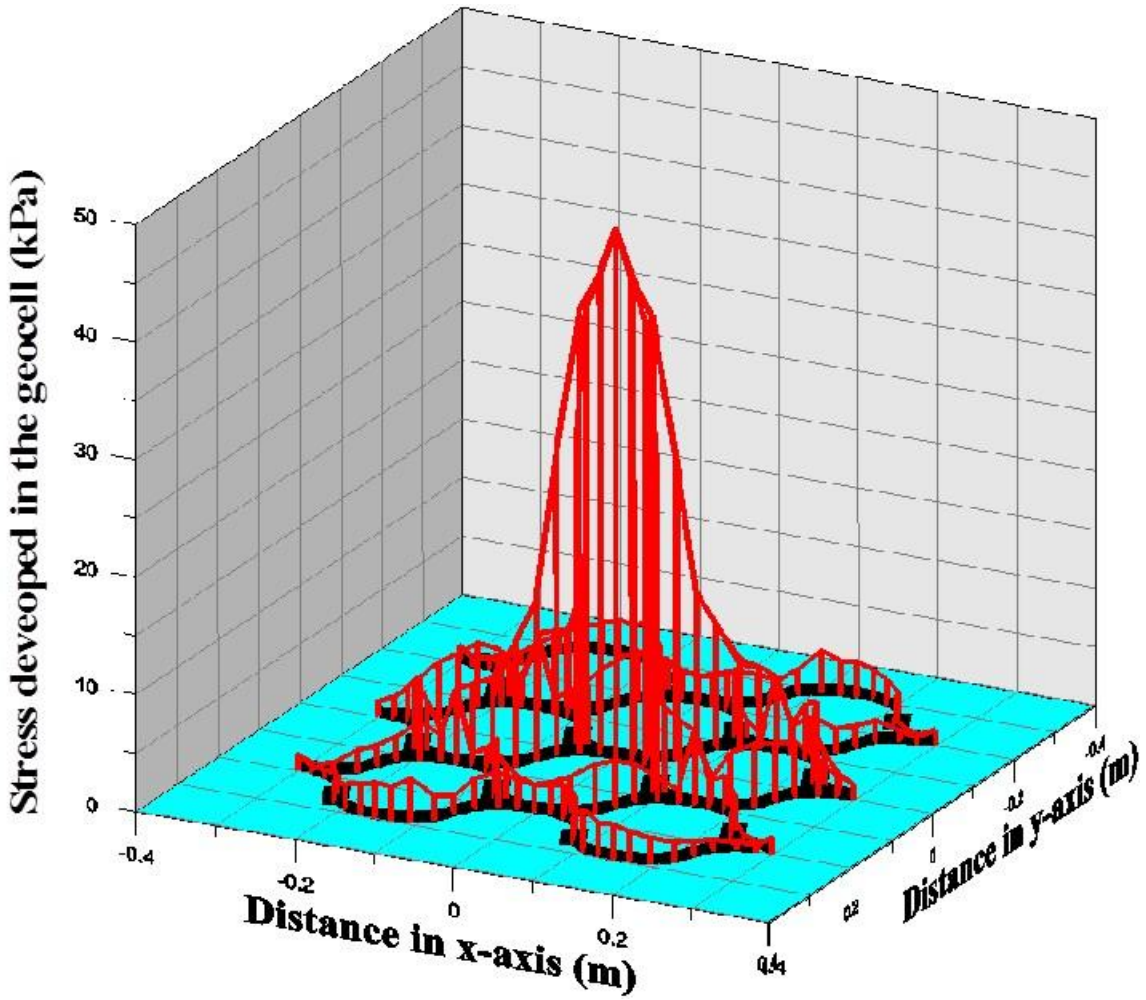

FIGURE 11 Confining stress developed in the geocell wall

CONCLUSIONS

This paper discusses the confinement mechanism of the geocell-reinforced dense sand bed overlying weak subgrade layer under monotonic loading through an extensive laboratory and numerical analysis. In this model, the soil layers were modeled using Mohr-Coulomb model and the geocell was modeled using linear elastic geogrid element. The honeycomb shaped geocell reinforcement was modeled and validated through the data obtained from the large scale experiments. The confining mechanism of geocell reinforcement was brought out by studying the mobilized stresses within the geocell walls as well as the infill soil under monotonic loading.

Geocell reinforced soil bed over weak sand subgrade has shown an improvement in the bearing capacity by about 25%, 40% and 55% at 3%, 5% and 10% rut depth ratios, respectively. Based on the horizontal stresses in the infill material, a two-fold higher horizontal stresses can be noticed in the geocell mattress compared to unreinforced sand beds. The increase in the horizontal stress is purely due to the lateral confinement offered by the geocell mattress to the infill soil.

The vertical stress distribution angle is found to be about 50^o to the horizontal or about 40^o to the vertical, which works out to be about 1.2:1 (V:H). About 92% vertical stress distribution is noticed in the case of geocell reinforced sand beds. The confining effect of the geocell mattress is measured and predicted through large scale tests and numerical simulations. Study brings out that the confining stress mobilized in the geocell mattress is not constant within the geocell pockets, but varies linearly along the height of the cell. The maximum confining stress is noticed at a height ratio h/D of 0.4 under the loading region. As high as 40 kPa of confining stress is mobilized in the geocell mattress under the loading with a highest confining pressure of 194 kPa in the infill soil.

For the design applications a linearly decreasing confining pressures within the cell pockets may be considered from the point of loading.

REFERENCES

1. Hegde, A., and Sitharam, T. G. 3-Dimensional numerical modelling of geocell reinforced sand beds. *Geotextiles and Geomembranes,* 2014, 43(2):171-181.
2. Rea, C., and Mitchell, J. K. Sand reinforcement using paper grid cells. Symposium on Earth Reinforcement, ASCE, Pittsburgh, 1978, 644-663.
3. Rajagopal, K., Krishnaswamy, N. R., and Latha, G. M. Behaviour of Sand Confined with Single and Multiple Geocells. *Geotextiles and Geomembranes*, 1999, 17, 171-184.
4. Krishnaswamy, N. R., Rajagopal, K. and Madhavi Latha, G. Model studies on geocell supported embankments constructed over soft clay foundation. *Geotechnical Testing Journal, ASTM*, 2000, 23:45-54.
5. Dash, S.K., Krishnaswamy, N. R. and Rajagopal, K. Bearing capacity of strip footings supported on geocell-reinforced sand. *Geotextiles and Geomembranes*, 2001, 19:235-256.
6. Wesseloo, J. *The Strength and Stiffness of Geocell Support Packs*, Ph.D. Dissertation, University of Pretoria, Pretoria, South Africa, 2004.
7. Sitharam, T. G., Sireesh, S., and Dash, S. K. Model studies of a circular footing supported on geocell-reinforced clay. *Canadian Geotechnical Journal*, 2005, 42, 693-703.
8. Madhavi Latha, G., Rajagopal, K., and Krishnaswamy, N. R. Experimental and Theoretical Investigations on Geocell-Supported Embankments. *International Journal of Geomechanics*, 2006, 6(1):30-35.
9. Pokharel, S. K., Han, J., Leshchinsky, D., Parsons, R. L., and Halahmi, I. Experimental evaluation of influence factors for single geocell-reinforced sand. Oral presentation and CD publication at the TRB 88th Annual Meeting, Washington, DC, 2009.
10. Hegde, A., and Sitharam, T. G. Experimental and numerical studies on footings supported on geocell reinforced sand and clay beds. *International Journal of Geotechnical Engineering*, 2013, 7(4):347-354.
11. Madhavi Latha, G., and Rajagopal, K. Parametric Finite Element Analyses of Geocell-Supported Embankment. *Canadian Geotechnical Journal*, 2007, 44(8):917-927.
12. Han, J., Yang, X., Leshchinsky, D., and Parsons, R. L. Behavior of geocell reinforced sand under a vertical load. *Transportation Research Record:*

Journal of the Transportation Research Board, No. 2045, Transportation Research Board of National Academies, Washington, D.C., 2008, 95-101.

13. Sireesh, S., Gowrisetti, S., Sitharam,T. G., and Puppala, A.J. Numerical simulations of sand and clay. *Ground Improvement*, 2009, 162(GI4):185-198.
14. Yang X., *Numerical Analyses of Geocell-Reinforced Granular Soils under Static and Repeated Loads*, Ph.D. Dissertation, University of Kansas, Kansas, USA, 2010.
15. Hegde, A., and Sitharam, T. G. Effect of infill materials on the performance of geocell reinforced soft clay beds, *Geomechanics and Geoengineering: An International Journal*, 2015, 10(3):163-173.
16. Sireesh, S., Sitharam, T. G., and Dash, S. K. Bearing capacity of circular footing on geocell sand mattress overlying clay bed with void. *Geotextiles and Geomembranes*, 2009, 27 (2):89-98.
17. Dash, S.K., Sireesh, S., and Sitharam, T.G. Model studies on circular footing supported on geocell reinforced sand underlain by soft clay. *Geotextiles and Geomembranes*, 2003, 21:197-219.
18. Sitharam, T. G. and Sireesh, S. Behaviour of embedded footings supported on geogrid-cell reinforced foundation beds. *Geotechnical testing Journal, ASTM*, 2005, 28, 452- 463.
19. Meyerhof, G. G. Ultimate bearing capacity of footings on sand layer overlying clay, *Canadian Geotechnical Journal*, 1974, 11(2):223-229.
20. Neto, A. J. O., Bueno, B. S. and Futai, M. M. A bearing capacity calculation method for soil reinforced with a geocell. *Geosynthetics International*, 2013, 20(3):129–142.
21. Leshchinsky, B and Ling, H. Effects of Geocell Confinement on Strength and Deformation Behavior of Gravel, *Journal of Geotechnical and Geoenvironmental Engineering*, 2013 , 139(2):340-352.
22. Hegde, A., and Sitharam, T. G. 3-Dimensional Numerical Analysis of Geocell Reinforced Soft Clay Beds by considering the actual geometry of Geocell Pockets. *Canadian Geotechnical Journal*, 2015, 52:1-12.